Non-linear Slack-Mooring Modelling of a Floating Two-Body Wave Energy Converter

Pedro C. Vicente[#1], António F. O. Falcão[#2], Paulo A.P. Justino[*3]

 # IDMEC, Instituto Superior Técnico,Technical University of Lisbon, Lisbon, Portugal

[1]pedro.cabral.vicente@ist.utl.pt

[2]antonio.falcao@ist.utl.pt

** Laboratório Nacional de Energia e Geologia, Lisbon, Portugal*

[3]paulo.justino@lneg.pt

***Abstract*— Most floating oscillating-body wave energy converters that have been proposed and developed so far are two-body systems where the power is extracted from the relative translational motion between the two bodies. As any floating device, floating point absorbers are subject to drift forces due to waves, currents and wind, and therefore need to be kept in place by a proper mooring system. The mooring cables can be approximately modelled as catenary lines in a quasi-static analysis. The use of a time-domain analysis allows for nonlinear mooring forces of slack chain cables to be considered. Numerical results for motion, mooring tensions and absorbed power are presented for a two body system consisting of a hemispherical floater and a submerged body and slack bottom moorings, for regular and irregular waves. Comparisons are given with the unmoored two-body heaving system, the moored heaving two-body system and with the simplified one body linear PTO model. Results show the possibility of occurrence of low-frequency horizontal oscillations of large amplitude, and non linear motions, even for regular waves. Some differences are seen in comparison with the simplified one body model and with the heave two-body system. The moorings were found not to affect very significantly the power absorbed.**

***Keywords* — Wave energy; Wave power; Arrays; Moorings; Point absorbers.**

I. INTRODUCTION

Floating point absorbers are a wide class of wave energy converters (WECs), developed initially in the late 1970s, for offshore deployment. They are oscillating bodies with small horizontal dimensions in comparison with the wavelength and their rated power ranges from tens to hundreds of kW. Examples of some devices, that reached the stage of prototype tested in the sea, are IPS buoy [1], Aquabuoy [2], Wavebob [3] and PowerBuoy [4].

In the numerical modelling of these devices, the assumption of a single-body WEC whose power take-off system (PTO) is activated by its heave motion is usually adopted to reduce the complexity of the theoretical and numerical modelling. In reality, most floating oscillating-body wave energy converters that have been proposed and developed so far are in fact two-body systems.

Devices like the IPS buoy, consisting of a floater rigidly connected to a long submerged vertical acceleration tube open at both ends within which a piston can slide, can be modelled as a two-body oscillating body converter, where the power is extracted from the relative translational motion between the two bodies. The dynamics of a two-body heaving wave energy converter has been theoretically analyzed in detail by Falnes [5] and numerically by several authors [6]-[8].

Also, as any floating device, floating point absorbers are subject to drift forces due to waves, currents and wind, and therefore need to be kept in place by a proper mooring system. Although similarities can be found between the energy converters and floating platforms, WECs mooring design have some important differences, since the mooring connections may significantly modify the energy absorption by the converter by interacting with its oscillations [9].

Different options exist for a mooring design and configuration. They can either be single slack chain catenary cables or taut synthetic mooring lines and can also have additional intermediary sinkers or floaters. Slack chain catenary lines rely on their weight to provide the necessary horizontal restoring force and, although they induce some vertically downward force, they allow for systems with a lower stiffness than the ones with taut synthetic lines.

The mooring, especially the slack-mooring, of (individual) floating wave energy converters has been addressed in the last few years by several authors (e.g. [9]-[14]). Fitzgerald and Bergdahl [13] studied in detail the effect of the mooring connections upon the performance of a wave energy converter, by linearizing the mooring forces about the static condition, which conveniently allows a frequency-domain analysis to be applied.

In the present paper we use a time-domain, rather than a frequency domain, analysis, which allows nonlinear mooring forces of slack chain cables to be considered. The mooring cables are approximately modelled as catenary lines in a quasi-static analysis [9]. This simplified approach is applicable if we consider waves, body displacements and time steps to be small, as it is done here. This means that, in the relationship between mooring forces and body position, dynamic effects (namely cable inertia and viscous drag forces) are ignored but not the cable (submerged) weight per unit length.

Numerical results for motion, mooring tensions and PTO absorbed power, are presented for a two body system consisting of a hemispherical floater, a submerged body and

slack bottom moorings, in regular and irregular waves. Comparisons are also given with the unmoored two-body heaving system, the moored heaving two-body system and with the simplified one body linear PTO model.

Variations in mean surface level due to tides and drifting forces due to currents and wind are ignored, which is acceptable if considering small wave amplitudes as done here. Taking into account the spherical shape of the buoys and assuming the mooring lines and the PTO to be attached to the centres of the bodies, it can be considered that the only significant modes of oscillation are heave and surge.

II. Mathematical Model

We consider a hemispherical floater, moored to the bottom by catenary lines, as shown in plane view in Fig. 1. In the absence of waves, we assume that the centre of the floater lies on the free-surface plane, a vertical distance H from the bottom of the sea, and an initial horizontal distance $L_0 + L$ from the anchor point on the bottom, where L_0 is the length of the cable that initially lays on the seabed and L is the horizontal length of the hanging part of the cable, from the touchdown point to the converter. In Fig.1 an identical mooring line is on the right hand side of the converter. The mooring lines are in the vertical plane containing the direction of propagation of the incoming waves (*x*-positive direction). The two bodies have initially a vertical distance D between their centres.

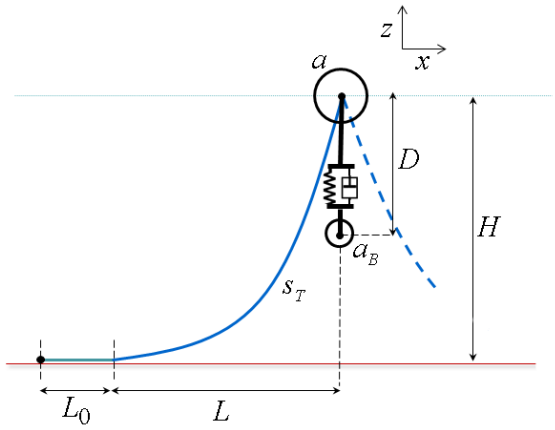

Fig. 1 Plane view representation of the slack chain moored two-body system.

In this analysis the slack mooring cables approximately modelled as catenary lines, are assumed inelastic and their dynamic effects (namely cable inertia and viscous drag forces) are ignored but not the submerged cable weight per unit length W, which depends on the cable material used (chain, wire, fibre) (see [9]). The classical catenary equations [15] apply, which can be written as

$$Z = \left(\frac{T_H}{W}\right)\cosh\left(\frac{X}{T_H/W} + \alpha\right) + \beta\,, \tag{1}$$

$$s = \left(\frac{T_H}{W}\right)\sinh\left(\frac{X}{T_H/W} + \alpha\right) + \gamma\,, \tag{2}$$

$$T = T_H \cosh\left(\frac{X}{T_H/W} + \alpha\right), \tag{3}$$

$$T_V = T_H \sinh\left(\frac{X}{T_H/W} + \alpha\right). \tag{4}$$

Here, X and Z are the horizontal and vertical coordinates of the cable point with respect to the lowest point of the catenary (where the cable departs from the bottom); α, β and γ are constants determined from boundary conditions; s is the length of the catenary-shaped part of the cable; T is the tension force on the cable, and T_H and T_V its horizontal and vertical components; W is the cable weight (minus buoyancy force) per unit length.

The boundary conditions at the point of seabed contact are $s = 0$, $X = 0$, $Z = 0$, $dZ/dX = 0$ and at the floater $X = L$ and $Z = H$. From these boundary conditions it is possible to calculate, for the initial equilibrium position, the initial horizontal cable tension T_H (which is the same at every point along the cable) and following that T_V and T. It is also possible to calculate the hanging cable length s, which in turn allows to calculate the necessary mooring cable length s_T to be used, $s_T = s + L_0$.

As for the submerged body, of radius of a_B and density ρ_B, its mass is

$$m_B = \tfrac{4}{3}\pi {a_B}^3 \rho_B\,, \tag{5}$$

which means that, if it is more dense or less dense than water, it will exert, respectively, a downwards or upwards force F_0 on the floater

$$F_0 = \tfrac{4}{3}\pi {a_B}^3 (\rho_B - \rho) g\,. \tag{6}$$

Since, in calm sea, the centre of the hemispherical floater (of radius a) is supposed to lie on the free-surface plane, and considering the two mooring lines as in Fig.1, its mass m must be

$$m = \frac{2}{3}\pi a^3 \rho - \frac{1}{g}(F_0 + 2T_V)\,. \tag{7}$$

Note that, since the buoy centre is assumed to lie on the free-surface horizontal plane in static conditions, the mass m of the moored buoy slightly varies with the system considered.

A. *Time Domain Analysis*

The buoy and bodies acted upon by the waves and mooring lines are made to oscillate in heave and horizontally. The displacements of their centres from their mean positions are defined by the coordinates (x_j, z_j) with $j = F$ for the floater, and $j = B$ for the submerged body and where x is the horizontal coordinate, and z is a vertical coordinate pointing upwards (see Fig.1).

The dynamic equations for the floater are then

$$(m + A_{\infty x})\ddot{x}_F(t) + \int_{-\infty}^{t} L_x(t-\tau)\ddot{x}_F(t)d\tau = f_{dx_F} + f_{PTO_X} + f_{MOO_X}\,, \quad (8)$$

$$(m + A_{\infty z})\ddot{z}_F(t) + \rho g S z_F(t) + \int_{-\infty}^{t} L_z(t-\tau)\ddot{z}_F(t)d\tau = f_{dz_F} + f_{\mathrm{PTO_Z}} + f_{\mathrm{MOO_Z}} + 2\mathrm{T_V}\,. \quad (9)$$

Here, $A_{\infty u}$ $(u = x,z)$ are the limiting values of the added masses $A_u(\omega)$ for $\omega = \infty$. For a hemispherical floater, it is $A_{\infty z} = \mu/2$ and $A_{\infty x} = 0.2732\mu$, where $\mu = 2\pi a^3\rho/3$ (see [16]). f_{dx} and f_{dz} are the horizontal (x) and vertical (z) components of the wave excitation force on the buoys (see [5]). Finally, $S = \pi a^2$.

The convolution integrals in Eqs. (8-9) represent the memory effect on the radiation forces. Their kernels can be written as

$$L_u(t) = \frac{2}{\pi}\int_{-\infty}^{t} \frac{B_u(\omega)}{\omega}\sin\omega t\, d\omega \quad (u = x,z)\,. \quad (10)$$

They decay rapidly and may be neglected after a few tens of seconds, which means the infinite interval of integration in Eqs. (8-9) may be replaced by a finite one in the numerical calculations (a 30s interval was adopted as sufficient). The integral-differential equations (8-9) were numerically integrated from given initial values of x, z, $\dot{x}$ and $\dot{z}$, with an integration time step of 0.05 s.

$B_u(\omega)$ $(u = x,z)$ are the frequency-dependent hydrodynamic coefficients of radiation damping concerning the horizontal (subscript x) and heave (subscript z) oscillation modes of the spherical buoys.

For the assumption of a single-body WEC whose PTO is activated by the floater heave motion, the force applied would simply be $f_{PTO_Z} = -Kz_F - C\dot{z}_F$ and $f_{PTO_X} = 0$. In the case of the two-body system, the force applied by the power take-off system (PTO) is proportional to the relative velocity between the two bodies.

We denote by $D + l(t)$ the cable length between the centres of the two bodies and easily find

$$l = \sqrt{(D + z_F - z_B)^2 + (x_F - x_B)^2} - D\,. \quad (11)$$

The angle α of the cable with the vertical direction is given by $\sin\alpha = (x_F - x_B)/(D + l)$. Assuming a linear spring of stiffness K and a (linear) damper force, we may write $f_{PTO} = -Kl - C\,dl/dt$. (The spring and damper are mounted in parallel.) The vertical force is $f_{PTO_Z} = f_{PTO}\cos\alpha$ and the horizontal force provided by the cable is $f_{PTO_X} = \mathrm{sign}(x_F - x_B) f_{PTO}\sin\alpha$.

The forces exerted by the mooring cables on the floater

$$f_{MOO_X} = -F_{X,A} + F_{X,B}\,, \quad (12)$$

$$f_{MOO_Z} = -(F_{Z,A} + F_{Z,B})\,. \quad (13)$$

are calculated based on the time varying values of the mooring forces $F_{X,v}$ and $F_{Z,v}$ on each cable, the one on the left $v = A$ and the one on the right $v = B$ side of the floater, and which are calculated, considering the cable length s defined for the static position, and the position of the floater at the previous instant of time, approximation which can be seen as valid since we consider a small time step. Similar catenary equations as before apply

$$H + z_j = \left(\frac{F_{X,v}}{W}\right)\cosh\left(\frac{D \pm x_j}{F_{X,v}/W} + \alpha\right) + \beta\,, \quad (14)$$

$$s = \left(\frac{F_{X,v}}{W}\right)\sinh\left(\frac{D \pm x_j}{F_{X,v}/W} + \alpha\right) + \gamma\,. \quad (15)$$

The plus or minus sign is to be chosen according to whether the cable considered is on the right or on the left side of the floater. Finally, T_V is, as already mentioned, the initial vertical cable tension applied at the buoy, at equilibrium position.

The submerged body is subject to the force exerted by the PTO, its own weight, the buoyancy force and the hydrodynamic forces on it. Dynamic equations, similar to the ones for the floater, apply

$$(m_b + A_{\infty Bh})\ddot{x}_B(t) + \int_{-\infty}^{t} L_{Bh}(t-\tau)\ddot{x}_B(t)d\tau = f_{d\,Bx} - f_{PTO_X} \quad (16)$$

$$(m_B + A_{\infty Bz})\ddot{z}_B(t) + \int_{-\infty}^{t} L_{Bz}(t-\tau)\ddot{z}_B(t)d\tau = f_{dBz} - f_{PTO_Z} \quad (17)$$

The kernels of the convolution integrals L_{Bu} $(u = x,z)$ are calculated as before, considering $B_{Bu}(\omega)$ $(u = x,z)$ as the hydrodynamic coefficients of radiation damping of the submerged body. f_{dBx} and f_{dBz} are the horizontal and vertical components of the wave excitation force on the body. Here we consider that the effects of the wave radiation and diffraction induced by the buoy upon the body are negligible. For the added mass $A_{\infty\,\mathrm{Bu}}$ $(u = x,z)$, we take the added mass of an accelerating sphere in an unbounded fluid (see e.g. [5]) $A_{\mathrm{Bx}} = A_{Bz} = (2/3)\rho\pi a_{\mathrm{B}}^3$.

III. Numerical results

We set $\rho = 1025$ kg.m^{-3} (sea water density) and $g = 9.8$ ms^{-2}. The submerged body is a sphere of density $\rho_{\mathrm{b}} = \rho_0$ (which means that $F_0 = 0$) and radius $a_B = 5$ m. The body submergence is assumed to be sufficient for the excitation force and the radiation damping on it to be neglected, i.e. we set $B_{\mathrm{Bx}} = B_{Bz} = 0$ and $f_{\mathrm{d\,Bx}} = f_{d\,Bz} = 0$.

In all cases for which results are shown here, it is $a = 7.5$ m, $D = 20$ m, $H = 60$ m, $L_0 = 0.80 \times L$ and $L = 60$ m. This results in a bottom-mooring cable of length

$s_T = 135.75$ m. A value for the submerged cable weight of $W = 1520$ N/m was used, adequate for example for a $d = 90$ mm thick chain cable (see [9]).

The values used for W, L and L_0 must be defined when designing the mooring system of (a specific) device for a given location accounting for the water depth and the expected maximum horizontal load at the site. The calculation done here are not for a specific site, but the mooring design values used here account for a maximum horizontal load of about 200 kN and a maximum horizontal motion of 12 m, which were both verified to be respected.

As for the PTO, we define $K = 0.1\rho g S = 175.5$ kN/m and $C = 251.1$kN/(m/s). The adopted value of C is obtained from $C = B$, and is the one that allows maximum wave energy absorption by an isolated unmoored hemispherical heaving buoy, at resonance frequency defined by resonance condition (see e.g. [17])

$$\omega = \left[\frac{m + A(\omega)}{\rho g S}\right]^{-1/2} . \qquad (18)$$

A. *Regular waves*

For regular waves the excitation force components are assumed to be simple-harmonic functions of time and so we may write $\{f_{dx}, f_{dz}\} = \mathrm{Re}\left(\{F_{dx}, F_{dz}\}e^{i\omega t}\right)$, where the complex amplitudes F_{dx} and F_{dz} are proportional to the amplitude A_w of the incident wave. The moduli of F_{dx} and F_{dz} may be written as $\{|F_{dx}|, |F_{dz}|\} = \{\Gamma_x A_w, \Gamma_z A_w\}$, where $\Gamma_x(\omega)$ and $\Gamma_z(\omega)$ are (real positive) excitation force coefficients.

Deep water was assumed for the hydrodynamic coefficients of added mass, radiation damping and excitation force. The frequency dependent numerical values were obtained with the aid of the boundary element code WAMIT, for the radiation damping coefficients $B_u(\omega)$ and the absolute value $\Gamma_u(\omega)$ and phase $\arg\left(F_{dz}(\omega)/F_{dx}(\omega)\right)$ of the excitation forces coefficients, for the floating hemispheres, oscillating horizontally and vertically ($u = h, z$).

Numerical results are presented in Figs 2 to 8 for regular waves of $A_w = 1$ m and $T = 8$ s. Comparisons are shown for identical floaters (with the same parameters except where otherwise stated), for the unmoored two-body heaving system, the moored heaving two-body system and with the simplified one-body linear PTO model.

Fig. 2 shows the heave and surge motion, of both the floater and the submerged body, for regular waves. It can be seen that the floater has large surge amplitude of motion and a heave motion with amplitude close to the wave amplitude. The heave motion of the submerged body has an amplitude which is higher than the one from surge and which is also higher than the amplitude heave motion of the floater. All motions except the floaters heave clearly present non linear or non simple harmonic oscillations.

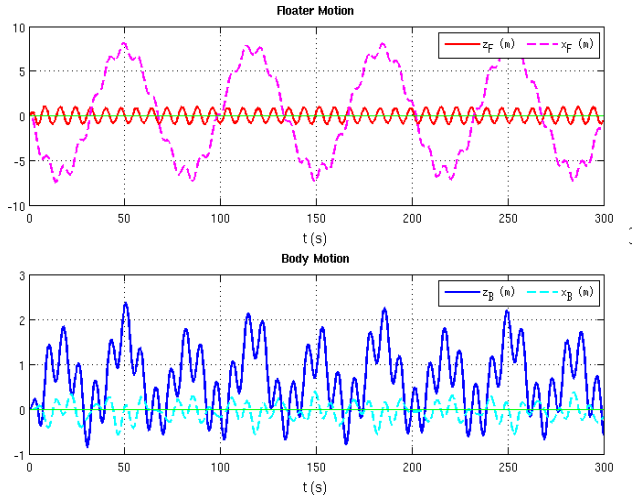

Fig. 2 Heave and surge motion, of both the floater and the submerged body, in regular waves $A_w = 1$m and $T = 8$s.

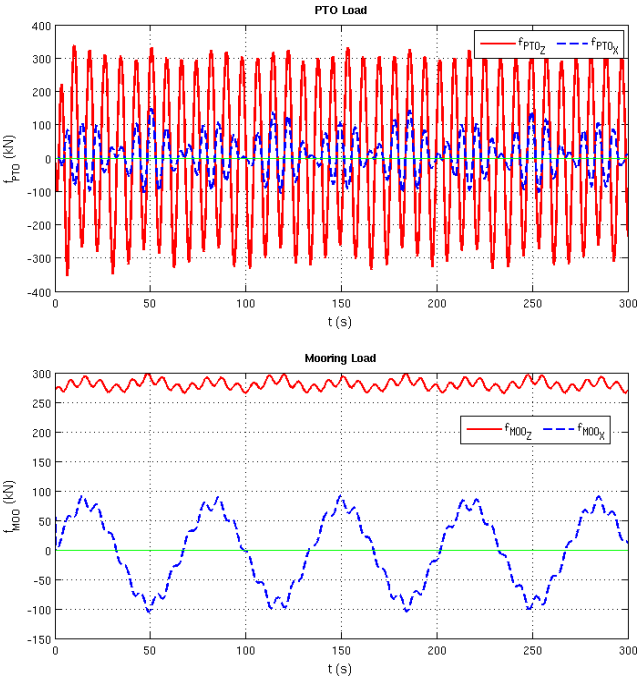

Fig. 3 Load applied to the moving floater. On top, the vertical f_{PTO_Z} (solid red line) and the horizontal load f_{PTO_X} (dashed blue line) from the PTO. Below, the vertical f_{MOO_Z} (solid red line) and horizontal f_{MOO_X} (dashed blue line) loads from the mooring cables, in regular waves $A_w = 1$m and $T = 8$s.

Fig. 3 shows, on the top, the load applied to the moving floater, the vertical f_{PTO_Z} (solid red line) and horizontal load f_{PTO_X} (dashed blue line) by the PTO, and, below, the vertical f_{MOO_Z} (solid red line) and horizontal f_{MOO_X} (dashed blue

line) loads from the mooring cables. It can be seen that the vertical load from the PTO is larger than the horizontal load (as expected) and similar behaviour occurs for the mooring loads. The non linear nature of the forces can be clearly seen, especially for the horizontal components, but also for the vertical mooring load.

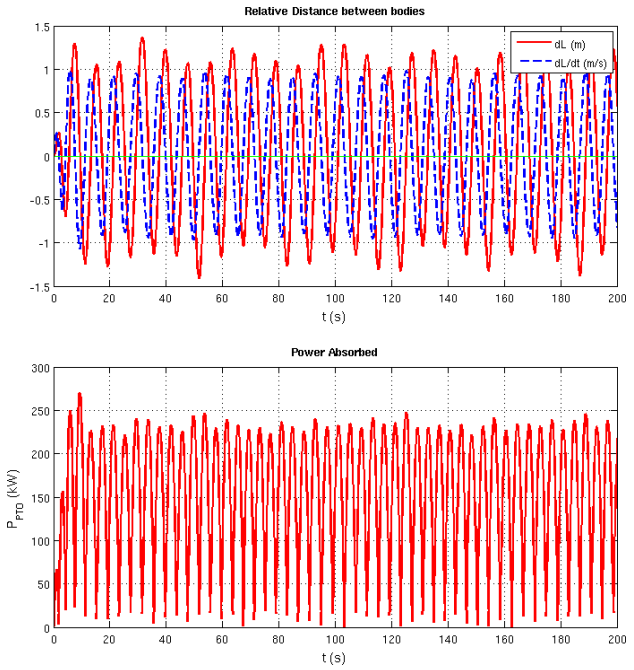

Fig. 4 On top, variation in the distance between the two bodies (l and dl/dt) and, below, the power extracted P_{PTO} from this motion, for regular waves $A_w = 1\text{m}$ and $T = 8\text{s}$.

Fig. 4 shows, on top, the variation in the distance between the two bodies (l and also dl/dt) and, below, the power extracted from this motion P_{PTO}. It can be seen that the cable length variation is almost harmonic but the horizontal motion introduces some slight non linear oscillation, which in the end affects, even if only slightly, the absorbed power.

TABLE I
SYSTEM PARAMETERS VARIATION INFLUENCE IN PERFORMANCE

	x_{Max}		$(P_{PTO})_{avg}$		$(f_{MOO})_{avg}$	
	–15%	+15%	–15%	+15%	–15%	+15%
D	1.00	1.00	1.00	1.00	1.00	1.00
ρ_B	0.97	1.02	1.18	0.85	1.00	1.00
a	0.90	1.05	0.49	1.87	0.98	1.01
C	0.99	1.00	0.88	1.12	1.00	1.00
K	0.99	1.01	0.95	1.05	1.00	1.00
L	0.72	1.35	1.00	1.00	1.32	0.83
d	1.16	0.88	1.00	1.00	0.74	1.30
A_w	0.86	1.14	0.72	1.32	0.99	1.01
T	0.95	1.02	0.94	1.13	0.99	1.00

Table 1 indicates what influence does a variation of 15% of the system parameters, has on the performance, in terms of maximum surge motion, average power absorbed and average mooring load. The values are a coefficient with regard with the case results presented previously: $D = 20\,\text{m}$, $\rho_b = \rho$, $a_B = 5\ \text{m}$, $a = 7.5\,\text{m}$, $K = 0.1\rho g S = 175.5\,\text{kN/m}$, $C = 251.1\,\text{kN/(m/s)}$, $H = 60\,\text{m}$, $L_0 = 0.80 \times L$, $L = 60\,\text{m}$. $d = 90\,\text{mm}$, $A_w = 1\,\text{m}$ and $T = 8\,\text{s}$. When one of the parameters is varied the remaining are maintained.

It can be seen that the parameters which appear to have a greater influence are the floater radius (on the power absorbed), the damping coefficient (also on power), the distance between the touchdown point and the floater and the thickness of the chain cable (both on the surge motion and the mooring forces) and finally the wave height and period (both mostly on the surge motion and the power absorbed).

Some comparisons are also made with other systems, with the moored heaving two-body system (where we considerer only vertical motion and have simply $f_{dx_F} = 0$), the unmoored two-body heaving system (where we have $f_{dx_F} = 0$ and $f_{MOO} = 0$ and $T_V = 0$) and with the simplified one body moored linear PTO model (where we have $f_{PTO} = -Kz_F - C\dot{z}_F$).

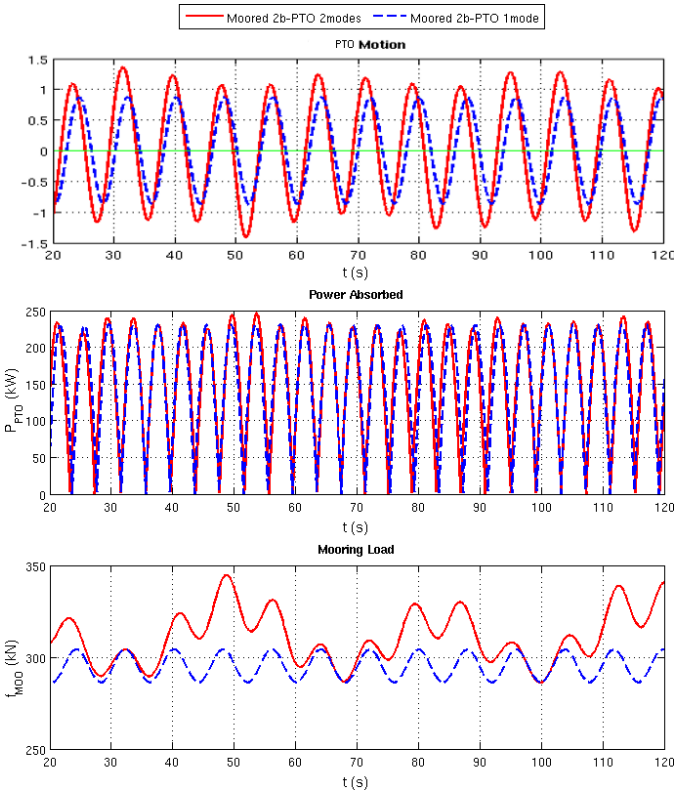

Fig. 5 Comparison between the moored two-body system with only heave motion (solid red line) and with heave and surge motion (dashed blue line), in terms of corresponding PTO motion (top), mooring loads (middle) and absorbed power (bottom), for regular waves $A_w = 1\text{m}$ and $T = 8\text{s}$.

Fig. 5 shows the comparison between the moored two-body system with only heave motion (solid red line) and the one with heave and surge motion (dashed blue line), in terms of corresponding PTO motion - z for the first case and dl/dt for the second (on the top), of the total mooring load on the converter (on the middle) and of the absorbed power (bottom). It can be seen that in terms of corresponding PTO motion and power absorbed the difference is very slight and there are only significant differences in the mooring load, as could be expected.

Fig. 6 shows the comparison of the heave motion (on top), and of the absorbed power (bottom), between the moored (solid red line) and the unmoored (dashed blue line) two-body heaving PTO system. It can be seen that there is only also a slight difference in motion and absorbed power when introducing the moorings.

Fig. 7 shows the comparison between the moored two-body system (solid red line) and the moored one-body system (dashed blue line), in terms of heave motion (top right), surge motion (top left), absorbed power (below right) and total mooring load on the converter (below left). It can be seen that there are only slight differences in term of motion and some differences in terms of mooring loads, but significant differences in terms of absorbed power.

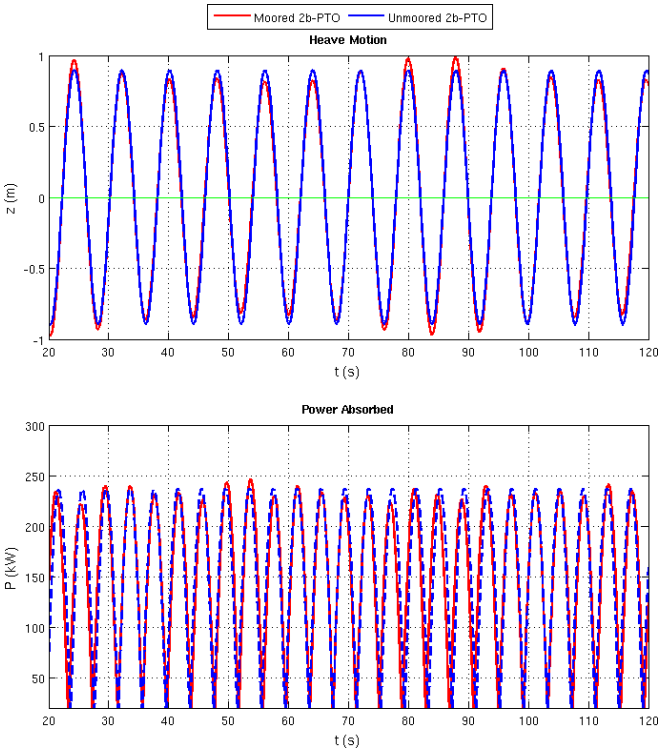

Fig. 6 Comparison of the heave motion (on top), and of the absorbed power (below), between the moored (solid red line) and the unmoored (dashed blue line) two-body PTO system, for regular waves $A_w = 1\text{m}$ and $T = 8\text{s}$.

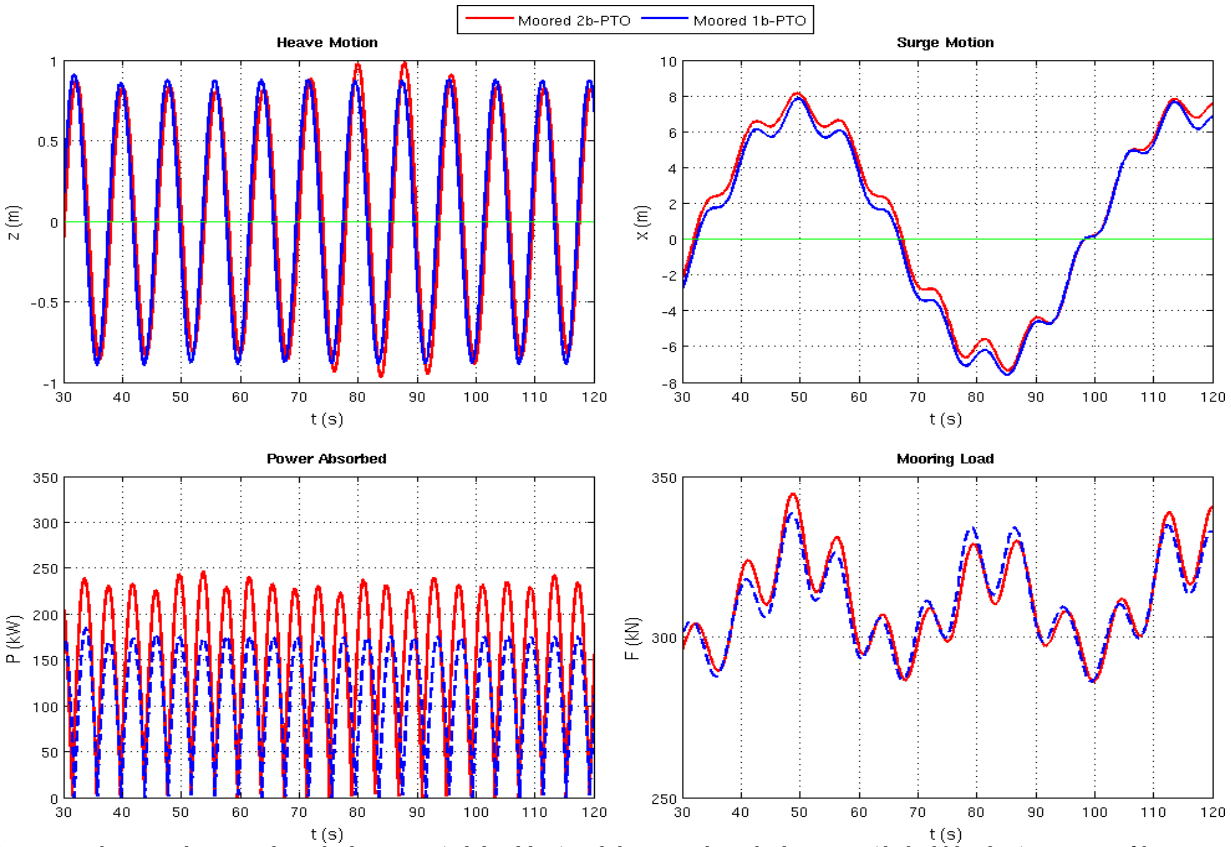

Fig 7 Comparison between the moored two-body system (solid red line) and the moored one-body system (dashed blue line), in terms of heave motion (top right), surge motion (top left), absorbed power (below right) and mooring loads (below left) , for regular waves $A_w = 1\text{m}$ and $T = 8\text{s}$.

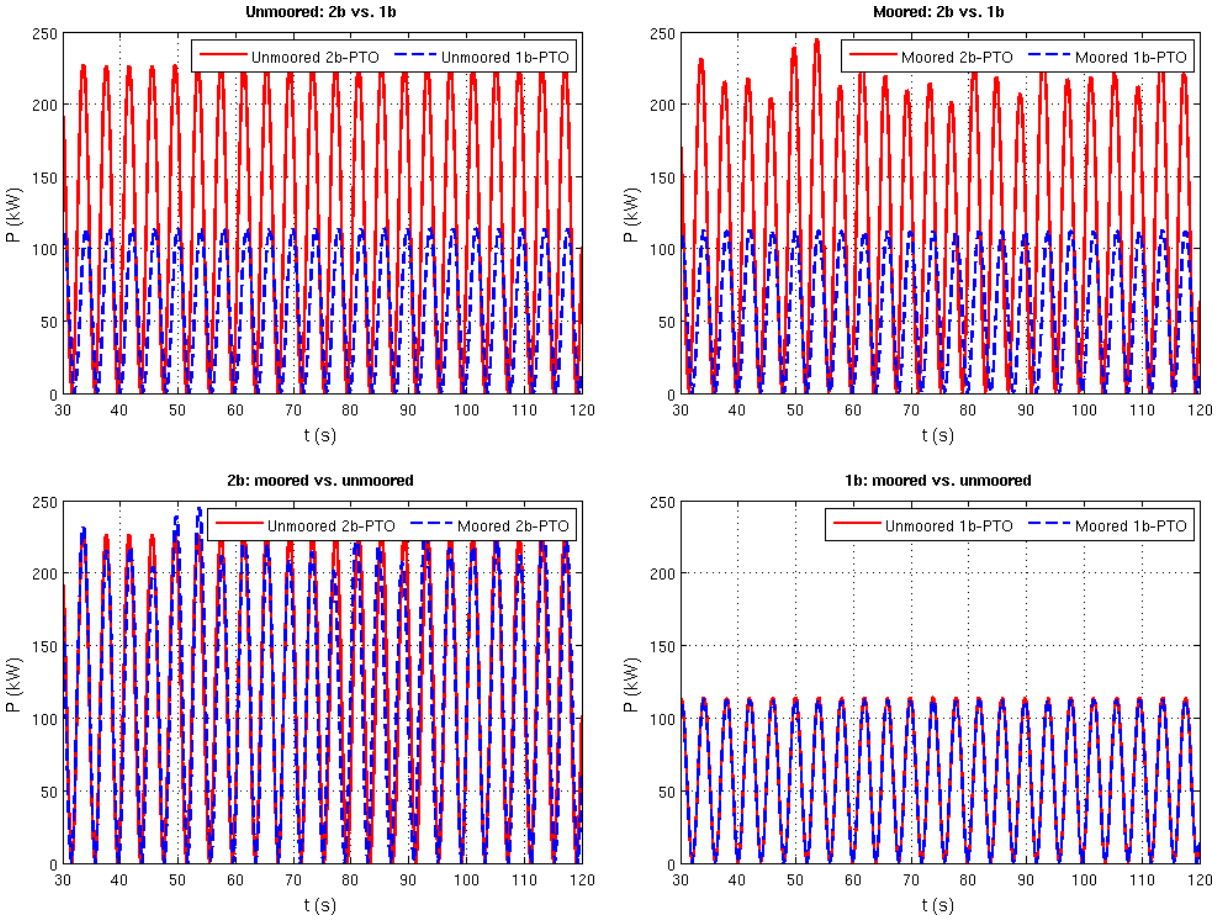

Fig 8 Comparison between the unmoored and moored and one-body and two-body system absorbed power, for regular waves $A_w = 1\text{m}$ and $T = 8\text{s}$.

Fig. 8 shows the comparison between the power absorbed by the unmoored and moored and the one-body and the two-body system. These figure gives an idea of the impact of considering a one-body or a two-body system, either unmoored or moored and also, of the impact of the mooring system either in a one-body or a two-body system. Differences can be seen between the different cases. It can be seen that there is some difference between considering a one-body system or a two-body system and that that difference is not influenced by whether the system is moored or not. It can also be seen that the mooring system has a small impact on the power absorption process, but that this influence may be more significant when considering a two-body rather than a one-body system. It should however be noticed that when we consider moorings we are in fact also taking into account the influence of the horizontal motions.

B. *Irregular waves*

Real irregular waves may be represented, in a fairly good approximation, as a superposition of regular waves, by defining a spectrum. Since our wave energy converter is axisymmetric and insensitive to wave direction, it is reasonable to assume the spectrum to be one-dimensional. We adopt the Pierson-Moskowitz spectral distribution, defined by (SI units, [18])

$$S_\varsigma(\omega) = 263 H_s^2 T_e^{-4} \omega^{-5} \exp(-1054 T_e^{-4} \omega^{-4}), \quad (19)$$

where H_s is the significant wave height and T_e is the energy period.

To obtain time-series of the water surface elevation at a point due to irregular waves representative of a particular sea state, various simulation methods can be applied. A commonly used method, assumes that a random Gaussian process can be obtained by the sum of a large number of N sinusoidal components with phases randomly generated and deterministic amplitudes derived from the density spectrum.

For time-series calculations, the spectral distribution is then discretized as the sum of a large number N of regular waves of frequency $\omega_n = \omega_0 + n\Delta\omega$, where ω_0 is the lowest frequency considered ($\omega_0 / \Delta\omega$ should be an irrational number in order to ensure the non-periodicity in the time-series), $\Delta\omega$ is a small frequency interval, $n = 0, 1, 2, \text{K}, N-1$, and the spectrum is supposed not to contain a significant amount of energy outside the frequency range $\omega_0 \le \omega \le \omega_0 + (N-1)\Delta\omega$. The (deterministic) amplitude of the wave component of order n is $A_{wn} = \left(2 S_\varsigma(\omega_n)\Delta\omega\right)^{1/2}$.

The excitation force may be written as

$$f_{du}(t) = \sum_n A_{wn}\,\mathrm{Re}\left\{F_{du}(\omega_n)\,e^{i(\omega_n t+\phi_n)}\right\} \qquad (22)$$

$(u = h, z)$. In the simulations we adopted $\omega_0 = 0.05 + \sqrt{6}$ rad/s, $\Delta\omega = 0.01$ rad/s and $N = 200$. The phase ϕ_n of each component was chosen as a random real number in the interval $(0, 2\pi)$ .Results are plotted in Figs. 9-12, for irregular waves of $H_s = 2$ m, $T_e = 8$ s. The parameters for the floater, moorings and PTO, are as defined for regulars waves.

Fig. 9 shows the heave and surge motion, of both the floater and the submerged body, for irregular waves. It can be seen that the floater surge oscillations are still higher than the remaining and that the heave motion from the submerged body is still higher than the one of the floater.

As in Fig.3, but for irregular waves, Fig. 10 shows, on the top, the load applied to the moving floater, the vertical f_{PTO_Z} (solid red line) and horizontal load f_{PTO_X} (dashed blue line) from the PTO, and below, the vertical f_{MOO_Z} (solid red line) and horizontal f_{MOO_X} (dashed blue line) loads from the mooring cables. It can be seen that PTO vertical load is quite larger than the horizontal one, which presents only a very slight variation. The loads from the moorings appear to have a smaller amplitude variation.

Fig. 11 shows, on top, the variation in the distance between the two bodies (l and dl/dt) and, below, the power extracted P_{PTO} from this motion, as in Fig.4 but this time for irregular waves. The power output is as could be expected for irregular waves.

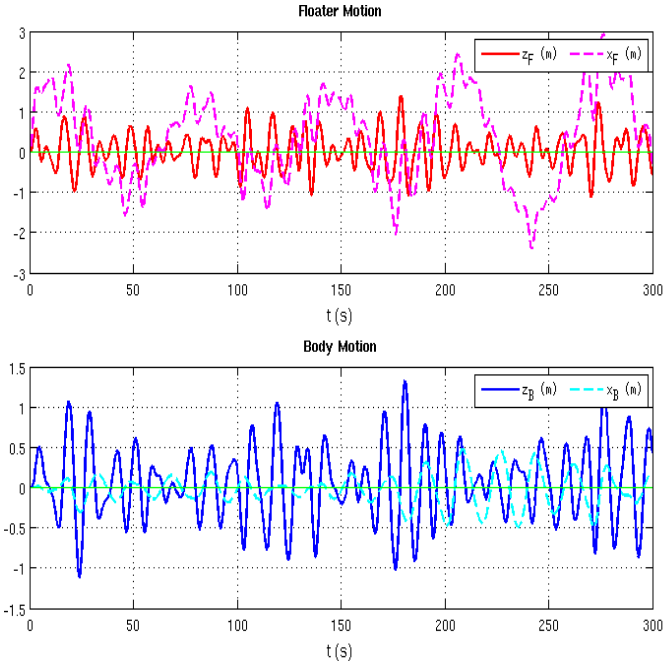

Fig. 9 Heave and surge motion, of both the floater and the submerged body, for irregular waves $H_s = 2$m and $T_e = 8$s .

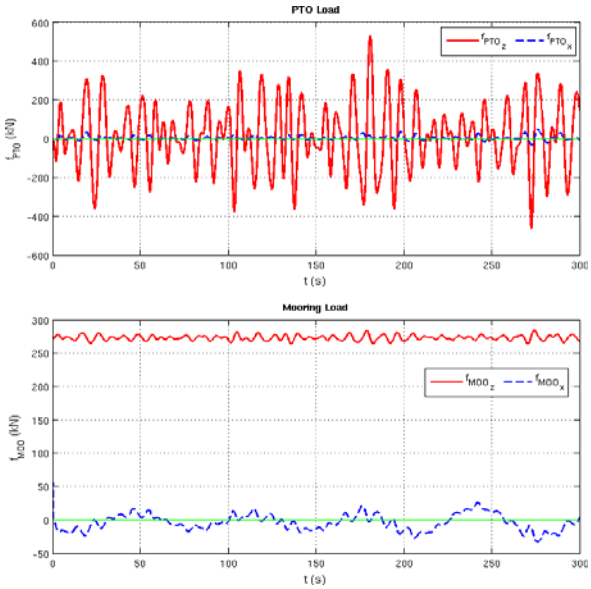

Fig. 10 Load applied to the moving floater, on top the vertical load (solid red line) and horizontal load (dashed blue line) from the PTO and below, the vertical load (solid red line) and the horizontal load (dashed blue line) from the mooring cables, for irregular waves $H_s = 2$m and $T_e = 8$s .

Finally, Fig. 12 shows the comparison between the power absorbed by the unmoored and moored and the one-body and the two-body system, for irregular waves. Similar differences as for regular waves can be seen, differences between the one-body and the two-body system, and a somewhat higher impact of the moorings in power absorption for the two-body than for the one-body system.

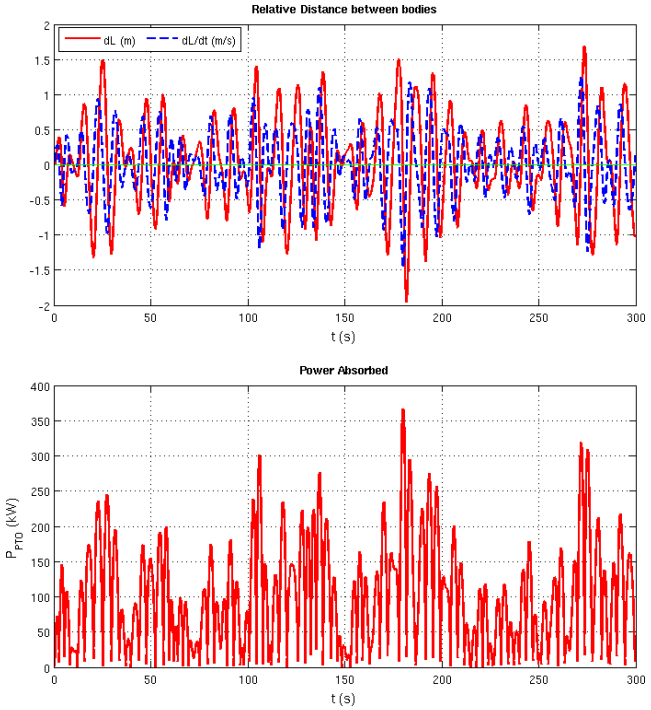

Fig. 11 On top, the variation in the distance between the two bodies (l and dl/dt) and, below, the power extracted P_{PTO} from this motion, for irregular waves $H_s = 2$m and $T_e = 8$s .

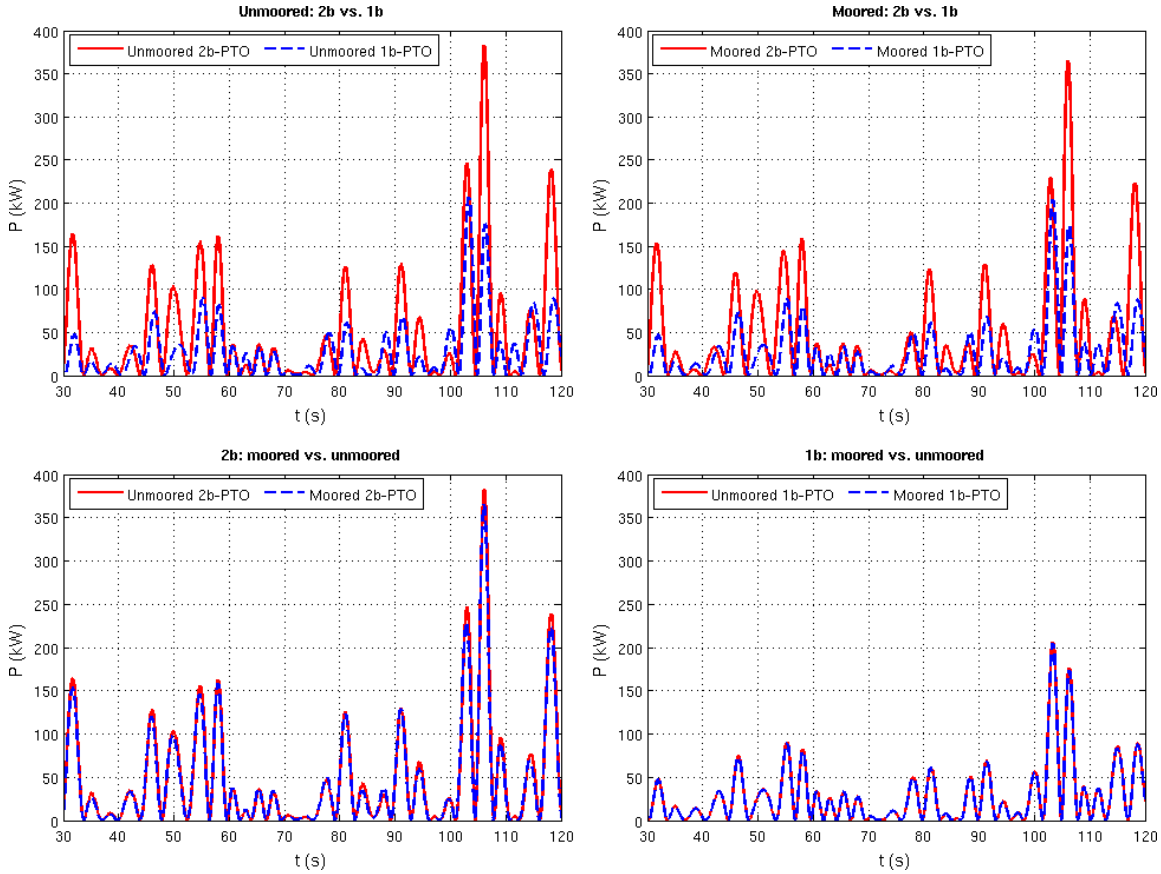

Fig 12 Comparison between the unmoored and moored and one-body and two-body system absorbed power, for irregular waves $H_s = 2\text{m}$ and $T_e = 8\text{s}$.

IV. Conclusions

A theoretical analysis was presented for the wave-induced heave and surge oscillations of a slack moored wave energy converter with a two body system consisting of hemispherical floater and submerged body and slack bottom moorings, for regular and irregular waves.

A time-domain analysis was used to take into account the nonlinear effects introduced by the mooring forces. The analysis focus on the amplitude of the motion of the converter, the load demands of the moorings and the power absorbed.

Curves were presented for certain given parameters and some comments were made on the behavior of the system. It is seen that the mooring cables introduce nonlinearities especially in the horizontal motion and horizontal mooring forces, but since we consider two modes of motion, this nonlinear behavior affects, even if only slightly, the absorbed power.

A brief analysis was made on the influence of the systems parameters through a 15% variation of their values. The impact of this variation on the maximum horizontal motion, power absorbed and mooring forces was analyzed. Some of the results may come as no surprise, but the magnitude of the influence should be taken into account.

Comparisons are also given with the unmoored two-body heaving system, the moored heaving two-body system and with the simplified one body linear PTO model. Some differences may be seen, mainly in terms of mooring loads and also power absorbed, when comparing the moored heaving two-body system with the simplified one body linear PTO model.

Although slack chain catenary lines rely on their weight to provide the necessary horizontal restoring force and although they induce some vertically downward force, they were found not to affect very significantly the power absorbed.

Acknowledgments

The work reported here was partly supported by the Portuguese Foundation for Science and Technology through their funding of IDMEC/LAETA, and under contracts PTDC/EME-MFE/103524/2008, POCI-SFA. The authors would also like to thank the anonymous reviewers for their comments.

References

[1] L. Cleason, J. Forsberg, A. Rylander, B. O. Sjöström, “Contribution to the theory and experience of energy production and transmission from the buoy-concept”, in *Proc. 2nd Int. Symp. Wave Energy Utilization. Trondheim, Norway*, p. 345-370, 1982.

[2] A. Weinstein, G. Fredrikson, M. J. Parks, K. Nielsen, “Aquabuoy, the offshore wave energy converter numerical modelling and optimization”,in *Proc. MTTS/IEEE Techno-Ocean ’04 Conf., Kobe, Japan*, vol. 4, p. 1854-1859, 2004.

[3] The Wavebob website. [Online]. Available: http://www.wavebob.com/

[4] The OPT website. [Online]. Available: http://www.oceanpowertechnologies.com/
[5] J. Falnes, *Ocean waves and oscillating systems: linear interactions including wave-energy extraction*. Cambridge University Press, 2002.
[6] G. S. Payne, J. R. M. Taylor, T. Bruce, P. Parkin, "Assessment of boundary-element method for modelling a free-floating sloped wave energy device. Part 1: Numerical modelling", *Ocean Engineering*, vol. 35, p. 333-341, 2008.
[7] S. J. Beatty, B. J. Buckham, P. Wild, "Frequency response tuning for a two-body heaving wave energy converter", in *Proceedings of 18th International Offshore and Polar Engineering Conference, Vancouver*, p. 342-348, 2008.
[8] R. P. F. Gomes, J. C. C. Henriques, L. M. C. Gato, A. F. O. Falcão, "IPS 2-body wave energy converter: acceleration tube optimization", *International Journal of Offshore and Polar Engineering*, vol. 20, p. 247-255, 2010.
[9] I. Johanning, G.H. Smith, J. Wolfram, "Mooring design approach for wave energy converters", in *Proc Inst Mech Eng Part M-J Eng Marit Environ*, vol. 220, p. 159-174, 2006.
[10] I. Johanning, G. H. Smith, J. Wolfram, "Towards design standards for WEC moorings", in *Proc 6th European Wave Tidal Energy Conf, Glasgow, 2005*.
[11] I. Johanning, G. H. Smith, J. Wolfram, "Interaction between mooring line damping and response frequency as a result of stiffness alterations in surge", in *Proc 25th Int Conf Offshore Mechanics Arctic Eng (OMAE 2006), Hamburg, 2006*, paper 2006-92373.
[12] J. Fitzgerald, L. Bergdahl, "Considering mooring cables for offshore wave energy converters", in *Proc 7th European Wave Tidal Energy Conf, Porto, Portugal, 2007*.
[13] J. Fitzgerald, L. Bergdahl, "Including moorings in the assessment of a generic offshore energy converter: a frequency domain approach", *Mar Struct*, vol. 21, p. 23-46, 2008.
[14] N. Fonseca, R. Pascoal, T. Morais, R. Dias, "Design of a mooring system with synthetic ropes for the FLOW wave energy converter", in *Proc 28th Int Conf Ocean Offshore Arctic Eng, Honolulu, Hawaii, 2009*, paper OMAE2009-80223.
[15] R. J. Smith, C. J. MacFarlane, "Statics of a three component mooring line", *Ocean Eng.*, vol. 28, p. 899-914, 2001.
[16] A. Hulme, "The Wave Forces Acting on a Floating Hemisphere Undergoing Forced Periodic Oscillations", *J. Fluid Mech*., vol. 121, p. 443-463, 1982.
[17] J. Lighthill, *An Informal Introduction to Theoretical Fluid Mechanics,* Oxford University Press, Oxford, 1986.
[18] Y. Goda, *Random Seas and Design of Maritime Structures*, 2nd edition, World Scientific, Singapore, 2002.